Inorganic Chemistry
including bioinorganic chemistry
Inorg. Chem., 1997, 36(24), 5440-5448, DOI:10.1021/ic970834r

Table S1. Kinetic characteristics of Cr(VI) reactions with As(III) in carboxylate buffers (pH 3.5).[a,b]

Buffer system[c]	Cr(VI) + As(III) + buffer[d]		Cr(VI) + buffer[e]	Reaction type[f]
	k_1, s^{-1}	k_2, s^{-1}	$10^3 \times k$, s^{-1}	
I	0.51	2.1×10^{-3}	0.2	A
II	0.46	2.8×10^{-3}	0.2	A
III	0.76	5.3×10^{-3}	0.2	A
IV	0.35	1.5×10^{-2}	0.3	B
V	0.82	5.0×10^{-2}	0.2	B
VI	0.50	6.2×10^{-2}	0.2	B
VII	0.38	0.89	10	B
VIII	0.22	2.0	4.9	B
IX	0.52		1.2	B
X	8.2×10^{-2}		0.2	B
XI	2.5×10^{-2}		3.7	C
XII	1.6×10^{-3}		~0.01	C
XIII	5.1×10^{-3}		0.03	C
XIV	3×10^{-4}		~0.01	C
XV	1.3×10^{-2}		10	C
XVI	1.6×10^{-3}		0.5	C

[a] $[Cr(VI)]_0 = 0.1$ mM, $[As(III)]_0 = 5$ mM, [buffer] = 100 mM, 1 M $NaClO_4$, 25°C. Deviations between the results of parallel kinetic experiments did not exceed 5 %.

[b] Analogous experiments were carried out at pH 2.5 and 4.5. Although values of the rate constants changed with pH, the reaction types (see note f) for all the studied systems remain unchanged.

[c] Designations of the buffer systems (see also note (1) in the main text): I - hmba; II - ehba; III - qa; IV - citrate; V - pic; VI - atrolactate; VII - *D*-gluconate; VIII - *D,L*-lactate; IX - ox; X - edta; XI - pyruvate; XII - mal; XIII - glycinate; XIV - *L*-prolinate; XV - salicylate; XVI - 100 mM acetate + 100 mM *D*-glucose.

[d] The kinetic data for the reactions in the buffer systems I-VIII were fitted by sequences of two pseudo-first order reactions: Initial → Intermediate → Product; k_1 and k_2 are the optimised rate constants. Reactions in the buffers IX-XVI led to Cr(VI) reduction to Cr(III) without the formation of observable intermediates; given in the table are the pseudo-first order rate constants for this process.

[e] Control reaction in the absence of As(III); k is the pseudo-first order rate constant for the reduction of Cr(VI).

[f] Designations of reaction types: *A* is the formation of relatively stable intermediates where the reductions of Cr(VI) by the buffer systems are negligible; *B* is the formation of unstable intermediates where the reductions of Cr(VI) by the buffer systems are negligible; *C* are where the rates of Cr(VI) + As(III) reactions are low or comparable with the rates of Cr(VI) + buffer reactions.

Table S2. Regeneration of Cr(VI) After the Decomposition of Cr(IV) Complexes[a]

Ligand	pH[b]	Yield of Cr(VI)[c]
ehba	2.8 - 3.2	90 ± 5
hmba	3.0 - 3.5	85 ± 5
qa	5.5 - 6.5	60 ± 5
pic	4.5 - 5.0	25 ± 5
ox	4.0 - 5.5	70 ± 5
mal	4.2 - 5.2	~100

[a] See Experimental Section for the conditions of the decomposition experiments.
[b] pH values of maximal stability for the corresponding Cr(IV) complexes (Figure 2).
[c] Percentage of theoretical yield according to eq 4. See Experimental Section for the procedure of determination of Cr(VI).

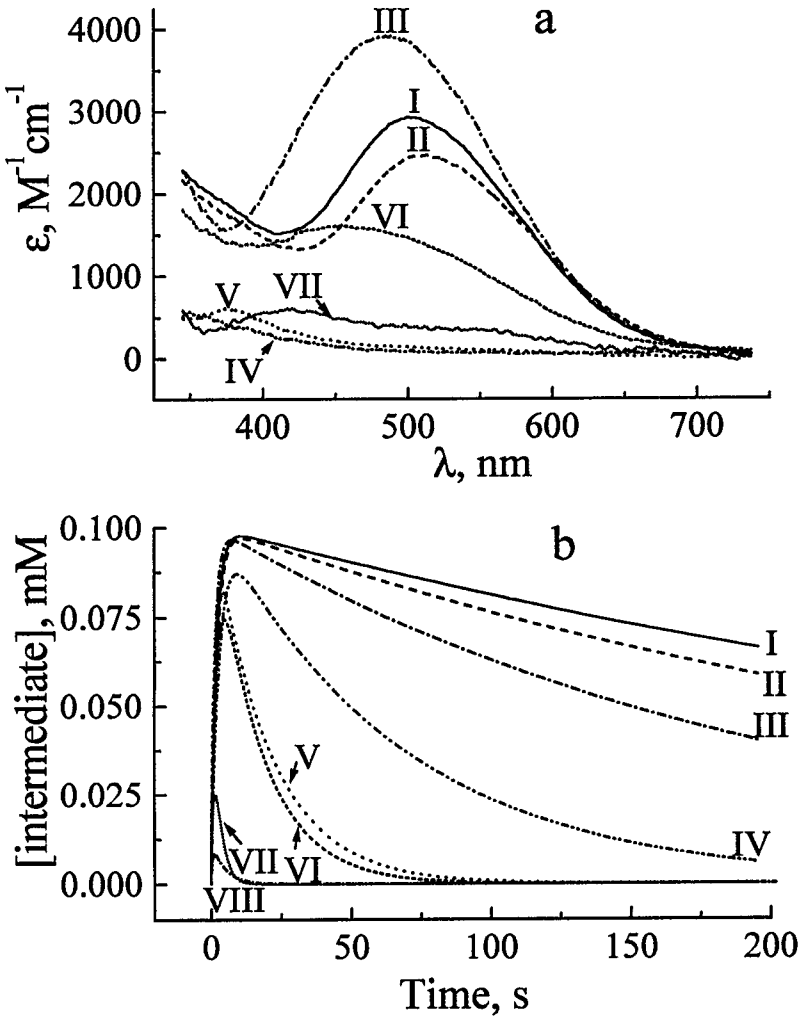

Figure S1. Results of the global kinetic analysis for the reaction Cr(VI) + As(III) + buffer (see Experimental Section for the conditions of Cr(IV) generation experiments); **(a)** estimated spectra of the intermediates; **(b)** concentration plots for the intermediates; designations of the buffers correspond to Table S1. The spectra for the buffers I, II, III and VI were attributed to Cr(IV) complexes. The spectra for the buffers IV, V and VII were attributed to the mixtures of Cr(III), Cr(V) and Cr(VI) complexes formed in the fast disproportionation of the initially formed Cr(IV) complex. No reliable spectra could be obtained in the case of the buffer VIII due to the very low concentration of the intermediate.

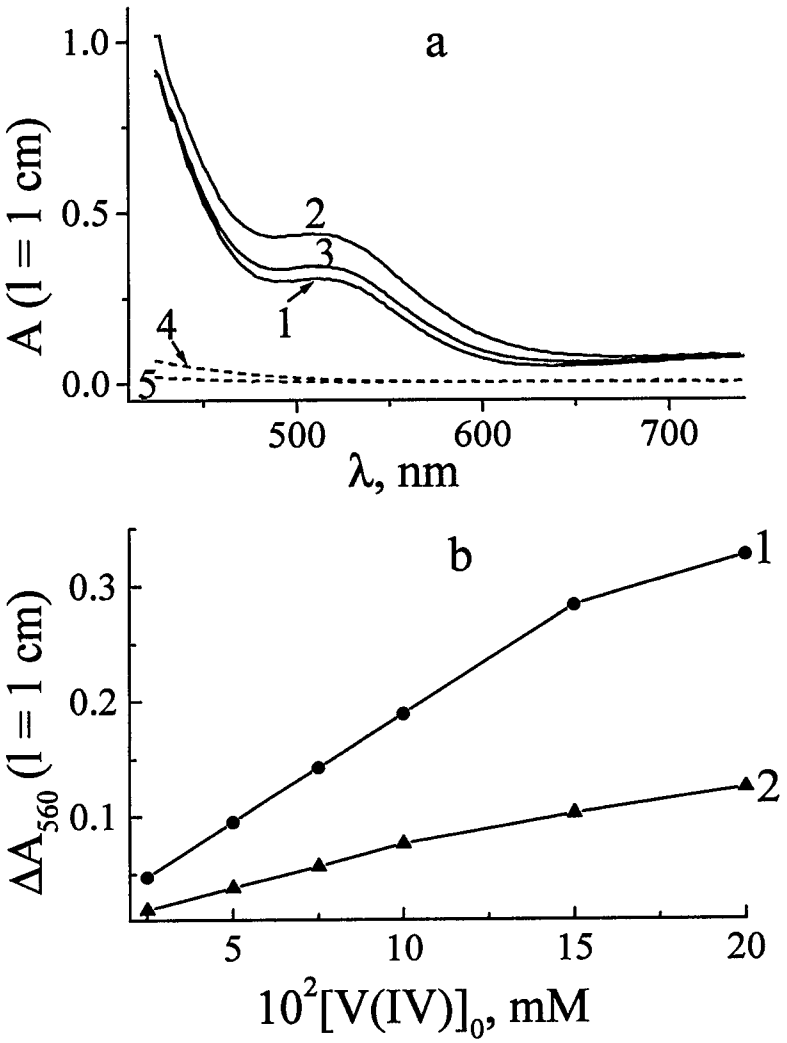

Figure S2. Typical results of the kinetic experiments for the reactions of 1 mM $Na[Cr^{V}O(ehba)_2]$ with 0.025-0.2 mM V(IV) in ehba buffers (pH = 3.5; 1 M $NaClO_4$; 25 °C); **(a)** typical spectral changes ($[V(IV)]_0$ = 0.05 mM): *1* is the spectrum of the reaction mixtures at $\tau = 0$ (practically independent on [ehba]); *2* and *3* are the spectra of the reaction mixtures after completion of the reaction (τ = 2 s) for [ehba] = 200 mM and 10 mM, respectively; *4* and *5* are the spectra of 0.05 mM V(V) in 200 mM and 10 mM ehba buffers, respectively; **(b)** changes of absorbance at 560 nm: *1*, [ehba] = 200 mM; *2*, [ehba] = 10 mM.

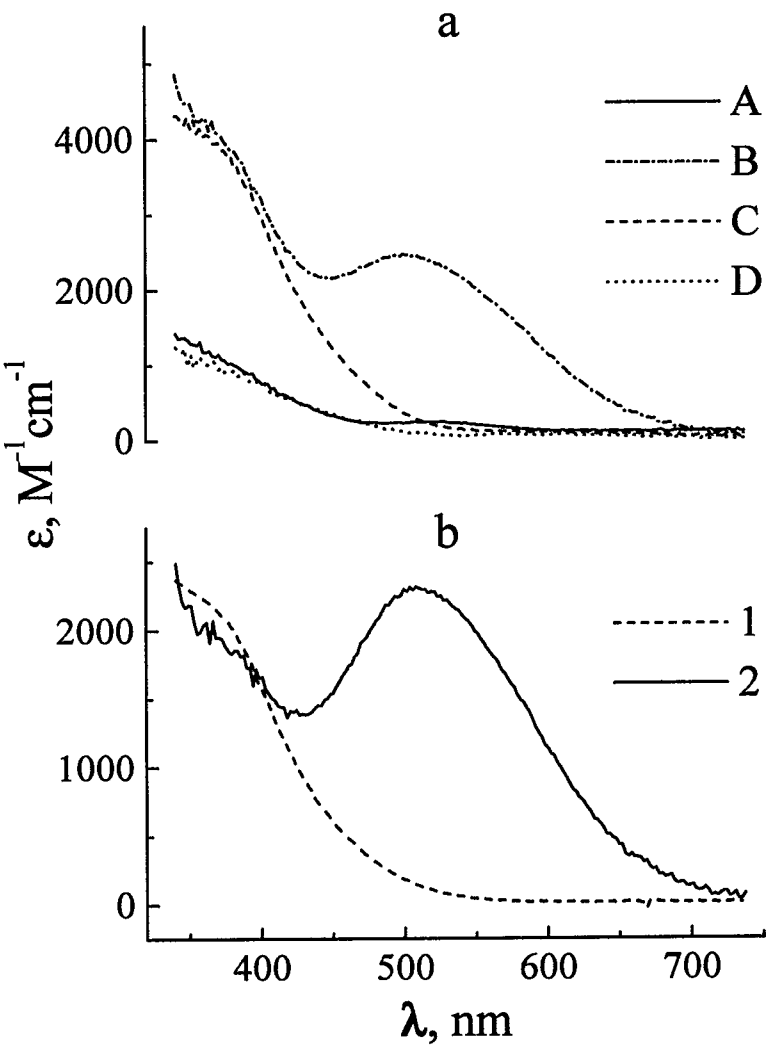

Figure S3. Typical results from the kinetic experiments involving the reactions of 0.1 mM $Na[Cr^{V}O(ehba)_2]$ with 2 mM V(IV) in 200 mM ehba buffer (pH = 3.5, 1 M $NaClO_4$; 25 °C); **(a)** spectra obtained by optimization of the reaction scheme $A \rightarrow B \rightarrow C \rightarrow D$. Attribution of the species: *A* = Cr(V)–ehba; *B* = Cr(IV)–ehba + V(V)–ehba; *C* = Cr(III)–ehba + V(V)–ehba; and *D* = Cr(III)–ehba + V(V)–V(IV)–ehba; **(b)** *1*: spectrum of V(V)–ehba, measured in a separate experiment; *2*: spectrum of Cr(IV)–ehba, obtained by substraction of the V(V)–ehba absorbance from the spectrum of the species *B*.

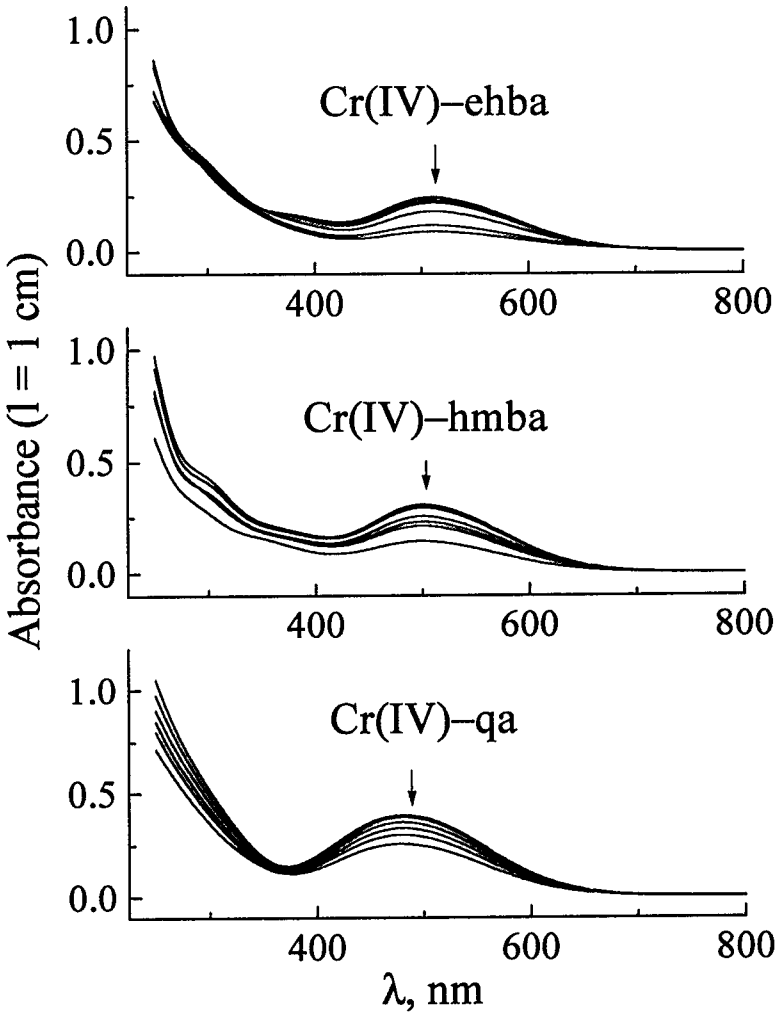

Figure S4. UV-visible spectra of Cr(IV)–Lig complexes at [Lig] = 200, 100, 50, 25, 15 and 10 mM ($[Cr(IV)]_0$ = 0.1 mM; pH = 3.5; $[NaClO_4]$ = 1 M; 25 °C.). The directions of spectral changes with decreasing [Lig] are shown by arrows.

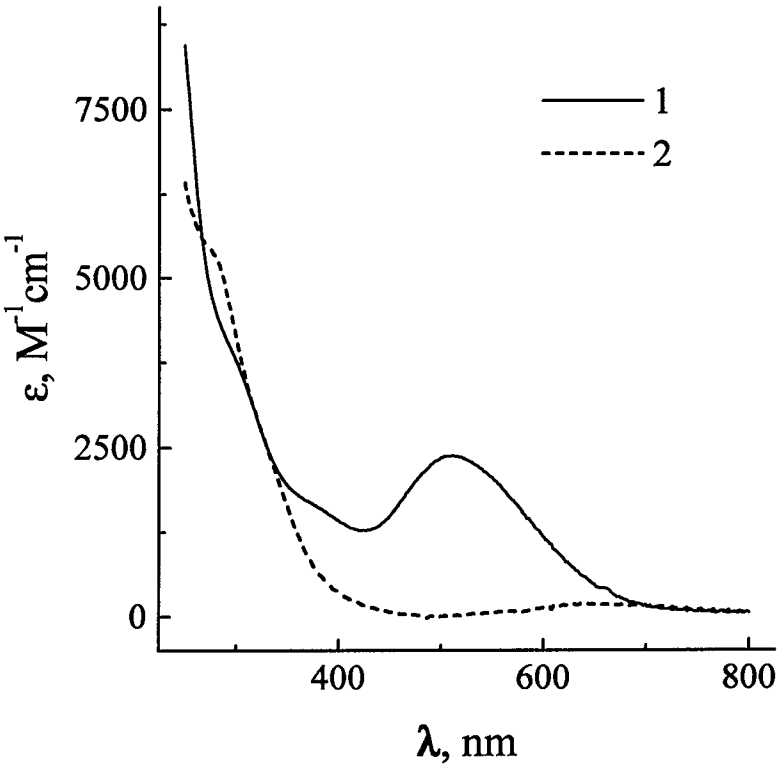

Figure S5. Estimated UV-visible spectra of Cr(IV)–ehba complexes **1** and **2** (eq 5, Scheme 1). Initial data for the estimations were the dependences of the spectra of Cr(IV)–ehba complexes on [Lig] and pH ($[Cr(IV)]_0$ = 0.1 mM; [Lig] = 10-200 mM; pH = 2.5-4.0; $[NaClO_4]$ = 1 M; 25 °C).

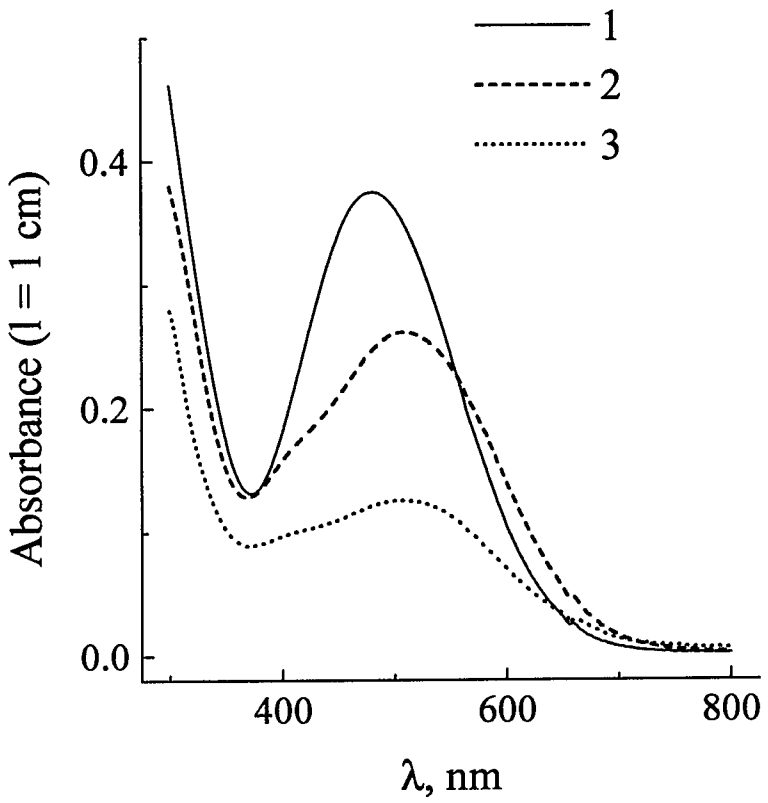

Figure S6. Influence of the mixing order to the generation of Cr(IV) complexes. *1*, Cr(IV)–qa complex: 44 mM qa buffer + 5 mM As(III) + 0.1 mM Cr(VI); reaction time 1 min. *2*, mixture of Cr(IV)–qa and Cr(IV)–ox complexes: Cr(IV)-qa complex generated as in *1*, then 13 mM ox added. *3*, mixture of Cr(IV) and Cr(III) complexes: 44 mM qa buffer + 13 mM ox buffer + 5 mM As(III) + 0.1 mM Cr(VI); reaction time 1 min. For all reactions: pH = 4.4; [$NaClO_4$] = 1 M; 21 °C. Concentrations of the reagents are estimated per volume of the final solutions.

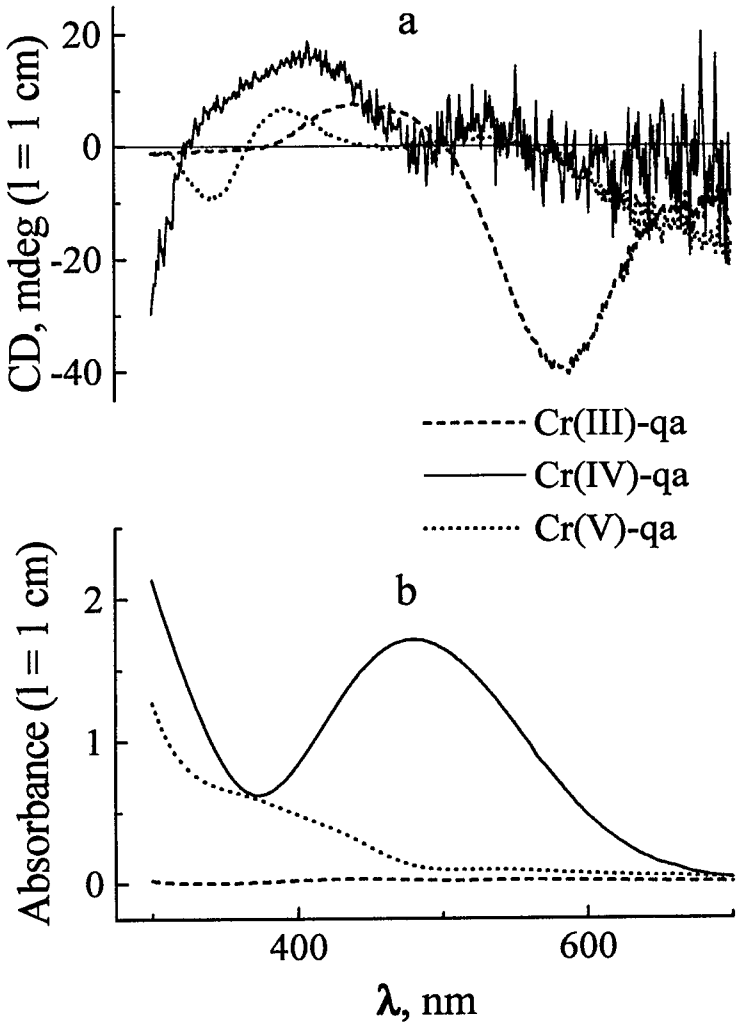

Figure S7. CD **(a)** and UV-visible **(b)** spectra of Cr(III), Cr(IV) and Cr(V) complexes with qa ligands ($[Cr(III)]_0$, $[Cr(IV)]_0$ or $[Cr(V)]_0$ = 0.5 mM; [Lig] = 50 mM; pH = 4.0; $[NaClO_4]$ = 1 M; 21 °C). The CD spectrum of Cr(IV)–qa is obtained in a single scan; the spectra of Cr(V)–qa and Cr(III)–qa are the averaged results of 10 scans (see Experimental Section for the conditions of CD spectroscopy).

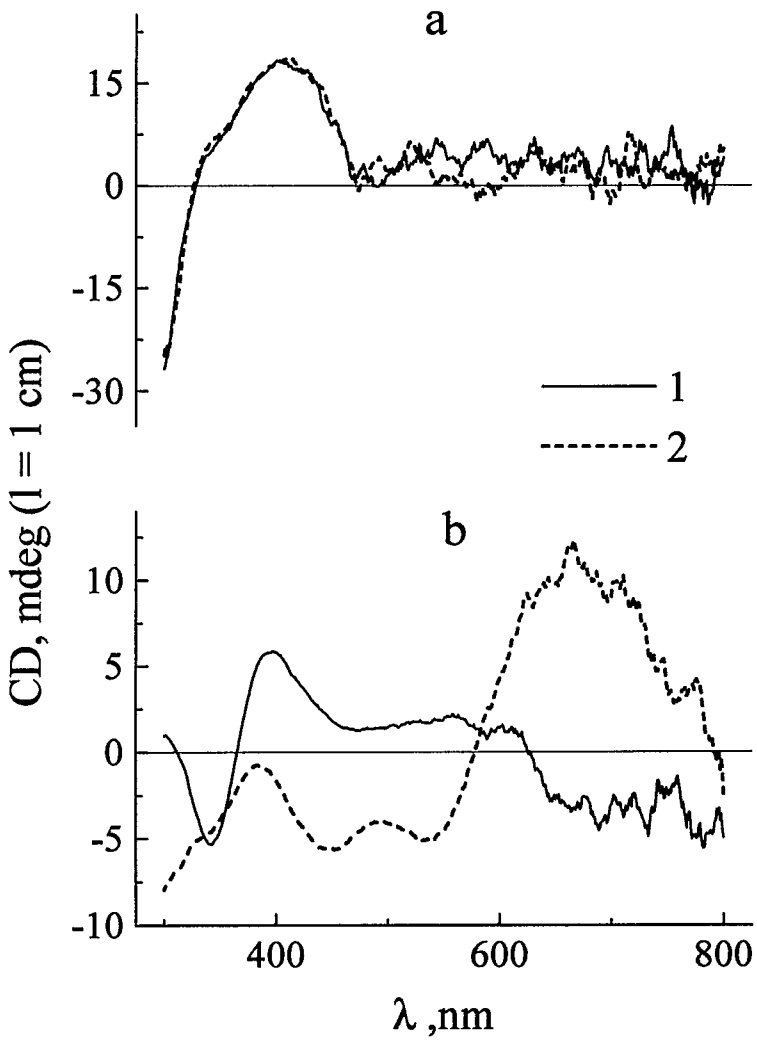

Figure S8. CD spectra of the Cr(IV)–qa **(a)** and Cr(V)–qa **(b)** complexes at pH = 3.5 (*1*) and 6.0 (*2*). $[Cr(IV)]_0$ or $[Cr(V)]_0$ = 0.5 mM; [Lig] = 50 mM; $[NaClO_4]$ = 1 M; 21 °C. The spectra are obtained by single scans (see Experimental Section for the conditions of CD-spectroscopy); noise reductions are performed by Origin software.

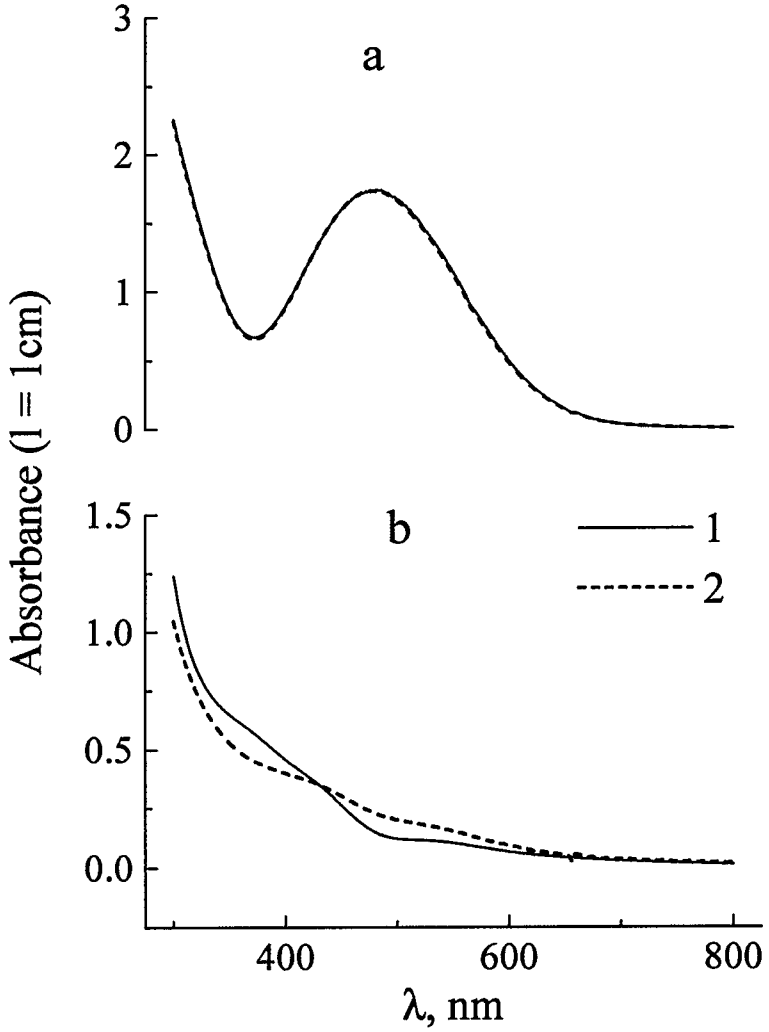

Figure S9. UV-visible spectra of Cr(IV)–qa **(a)** and Cr(V)–qa **(b)** complexes at pH = 3.5 (*1*) and 6.0 (*2*). Conditions correspond to Figure S8.

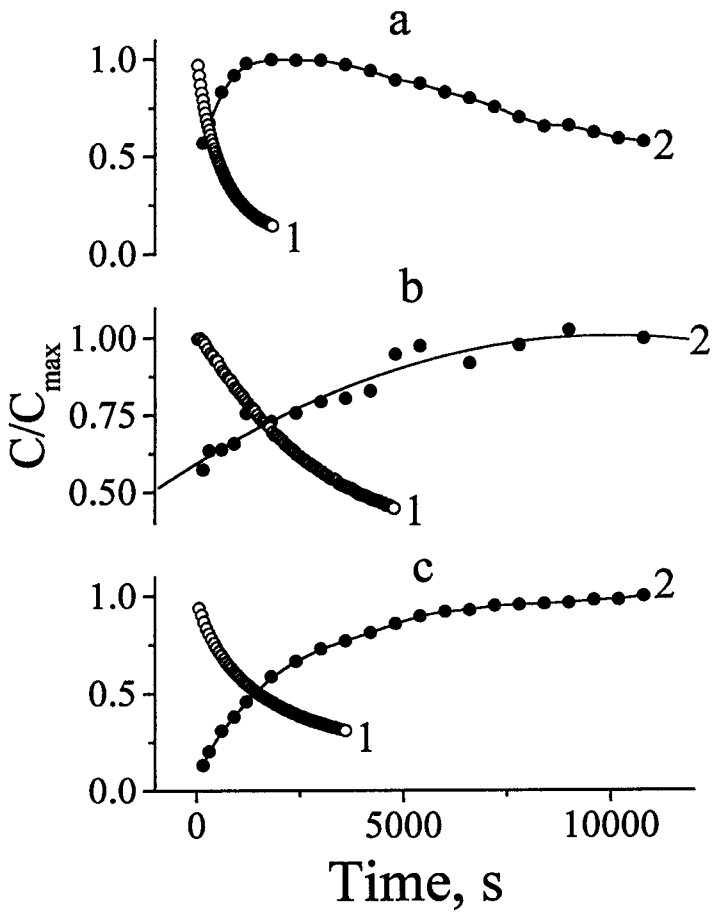

Figure S10. Comparison of concentration changes of Cr(IV) (*1*, followed by UV-visible spectroscopy at 550 nm) and Cr(V) (2, followed by EPR spectroscopy) in the reaction mixtures 0.1 mM Cr(VI) + 5 mM As(III) + 100 mM Lig (1 M $NaClO_4$, 21 °C). **(a)** Lig = qa, pH = 3.5; **(b)** Lig = qa, pH = 6.3; and **(c)** Lig = ehba, pH = 3.5.